Science and Technology Indonesia
e-ISSN:2580-4391 *p*-ISSN:2580-4405
Vol. 8, No. 2, April 2023

Research Paper

Facile Fabrication of Layered Double Hydroxide-Lignin for Efficient Adsorption of Malachite Green

Neza Rahayu Palapa[1*], Nur Ahmad[2,3], Alfan Wijaya[3], Zaqiya Artha Zahara[3]

[1]*Department of Chemistry, Faculty of Mathematics and Natural Sciences, Universitas Sriwijaya, Ogan Ilir 30662, Indonesia*
[2]*Graduate School, Faculty of Mathematics and Natural Sciences, Sriwijaya University, Ogan Ilir, 30662, Indonesia*
[3]*Research Center of Inorganic Materials and Complexes, Faculty of Mathematics and Natural Sciences, Sriwijaya University, Palembang, 30139, Indonesia*
***Corresponding author**: nezarahayu@gmail.com

Abstract
Preparation of layered double hydroxide-lignin (lignin-Zn/Al) carried out by coprecipitation method. The FTIR spectra of lignin-Zn/Al displayed at 3448, 2939, 1620, 1381, 1118, 1041, and 601 cm^{-1}. The characteristic peaks are located at 10.1°, 19.1°, 20.1°, 29.4°, 33.9°, and 60.4°. The lignin-Zn/Al nitrogen adsorption-desorption isotherm showed a Type-IV curve, indicating that it had a mesoporous structure. The H3 kind of hysteresis loop also provides evidence for the presence of mesopores within the lignin-Zn/Al complex. Lignin-Zn/Al, lignin, and Zn/Al had pHpzc values of 6.09, 3.01, and 6.09, respectively. Lignin-Zn/Al, lignin, and Zn/Al are positively charged when the pH of the solution is less than pHpzc, and they are negatively charged when the pH of the solution is more than pHpzc. The Langmuir and pseudo-second-order model best represented the MG adsorption onto all adsorbents. The lignin-Zn/Al, lignin, and Zn/Al were shown to have maximum Langmuir adsorption capacities of 83.034, 78.740, and 36.364 mg/g, respectively. Zn/Al adsorption capacity increased 2.28 times after being composited with lignin.

Keywords
Layered Double Hydroxide, Adsorption, Lignin, Malachite Green

Received: 20 January 2023, Accepted: 8 April 2023
https://doi.org/10.26554/sti.2023.8.2.305-311

1. INTRODUCTION

The contamination brought on by the wastewater discharge of organic dyes has become a more prominent issue because of the industry's rapid development (Tang et al., 2022). In many industries, including papers, tannery, printing inks, clothing, and others, dyes are widely utilized. As a result, a lot of colorful wastewater is produced, and many organic dyes will have a major harmful impact on the environment and human health (Giri et al., 2022; Vigneshwaran et al., 2021). Malachite green (MG), a triphenylmethane cationic dye, is frequently used in the textile industry (Jin et al., 2022). However, even at low concentrations, MG has been discovered to have numerous toxicological side effects on human bodies, such as mutagenic, teratogenic, and cancerous consequences (Buvaneswari and Singanan, 2022; Sarkar et al., 2021).

Several cutting-edge methods, such as extraction (Raval et al., 2022), photodegradation (Puthukkara et al., 2022), membranes (Iqbal et al., 2022), oxidation combining ultrasonic and electrochemical (Ren et al., 2021), and adsorption (Moradi and Panahandeh, 2022), have been used to remove MG from aqueous medium over the past few decades. Adsorption has garnered the most attention among these due to its straightforward functioning, design flexibility, practical recyclability, and excellent reliability. For the purpose of removing MG from an aqueous solution, numerous sophisticated adsorption materials have been developed recently, including Costus woodsonii (Van Tran et al., 2022), modified metal-organic frameworks (Dahlan et al., 2023), biowaste garlic peel (Pathania et al., 2022), and layered double hydroxide (Ahmad et al., 2023a). Layered double hydroxides (LDHs) are a type of 2D anionic clay that is composed of layers (Nazir et al., 2022). LDH has a structure similar to brucite with a large surface area, where M(II) is surrounded by six hydroxide ions, for instance, and forms an octahedral array that is connected to form an infinite 2D structure (Ahmed and Mohamed, 2022).

These adsorbents have excellent MG molecule adsorption performance, but for this purpose, sustainable, cost-effective adsorbents made from biomass are still required (Wang et al., 2018). Also, when compared to several previously described adsorbents, biomass-based adsorbents appear to be more environmentally friendly, cost-effective, and sustainable (Juleanti et al., 2021). Designing biomass-derived adsorbents to remove MG from aqueous media is therefore appealing. Lignin, an amorphous high-molecular aromatic polymer, is the second most prevalent biomass component on the planet after cellulose (Zong et al., 2023). The pulp and paper industry currently produces about 50 million tons of lignin as a byproduct each year. The vast majority of lignin that has been burned up to this point has been done so to create energy, which has resulted in significant lignin resource waste (Du et al., 2023). The use of inexpensive, readily available industrial waste lignin to produce effective functional materials for environmental remediation is a great solution when taking into account greater lignin usage and water remediation (Wang et al., 2022). A three-dimensional network structure and the abundance of functional groups that include oxygen in lignin give it more potential for functionalization (Hamad et al., 2022).

In this work, the coprecipitation technique was used to prepare the lignin-Zn/Al. Many cutting-edge characterization techniques were used to examine the physicochemical characteristics of lignin-Zn/Al. Also, the potential of lignin-Zn/Al was examined, as well as its application to simulated textile wastewater.

2. EXPERIMENTAL SECTION

2.1 Materials

All chemicals were used without any further purification. Sodium chloride, sodium hydroxide, aluminum nitrate nonahydrate, chloride acid, and zinc nitrate hexahydrate were purchased from Sigma Aldrich and Merck. Lignin and distilled water were purchased from Tokyo Chemical Industry and Brataco, respectively.

2.2 Preparation Lignin-Zn/Al and Characterization

Lignin-Zn/Al was prepared by the coprecipitation method. Both 0.25 M aluminum nitrate nonahydrate and 0.75 M zink nitrate hexahydrate were dissolved in 30 mL of distilled water, respectively. The solutions were added sodium hydroxide 2 M to pH 8 and stirred at 70°C for 4 h. Afterward, the Zn/Al added 3 g lignin was under continuous stirring for 3 days, filtered, and dried. The characterization of lignin-ZnAl using Fourier Transfer Infra-Red (FTIR) (Shimadzu), X-Ray Diffractometer (XRD) (Rigaku), and Surface Area Analyzer (Quantachrome).

2.3 Adsorption Process of MG

Batch adsorption tests were conducted in a shaker. Investigations were into the effects of temperature (30–60°C), initial dye concentration (60–100 mg/L), contact time (10–180 min), and pHpzc (2–11). Usually, 100 mL of beaker glass was filled with 30 mL of MG solution and 30 mg of lignin-Zn/Al. Liquid aliquots were obtained after adsorption and centrifuged. Then, the supernatant was examined using a UV-Vis spectrophotometer set to the maximum wavelength of 617 nm. Equation 1 was used to determine the concentration of MG.

$$q = \frac{(C_0\text{-}C)\times V}{m} \quad (1)$$

Where q is adsorption capacity at t time (mg/g); C_0 and C are initial concentration and concentration for t time of MG, respectively (mg/L); V is the volume of MG (L); m is the mass of lignin-Zn/Al (g).

3. RESULTS AND DISCUSSION

FT-IR spectra of Zn/Al, lignin, and lignin-Zn/Al were presented in Figure 1. The FTIR spectra of lignin-Zn/Al displayed at 3448, 2939, 1620, 1381, 1118, 1041, and 601 cm^{-1}. The stretching vibration of -OH from Zn/Al is responsible for appearing of the broad bandwidth 3448 and 1620 cm^{-1} (Ahmad et al., 2023b). The band at 2939 cm^{-1} is stretching vibration of aliphatic -CH from lignin and the distinctive peak at bandwidth 1381 cm^{-1} is anion interlayer NO_3^- from Zn/Al (Zubair et al., 2022). The peak at 1118 and 1041 cm^{-1} are ascribable to C-O and C-O-C from lignin, respectively (Sun et al., 2022). The metal oxide bond vibration is attributed to the band at 601 cm^{-1} (Chen et al., 2022).

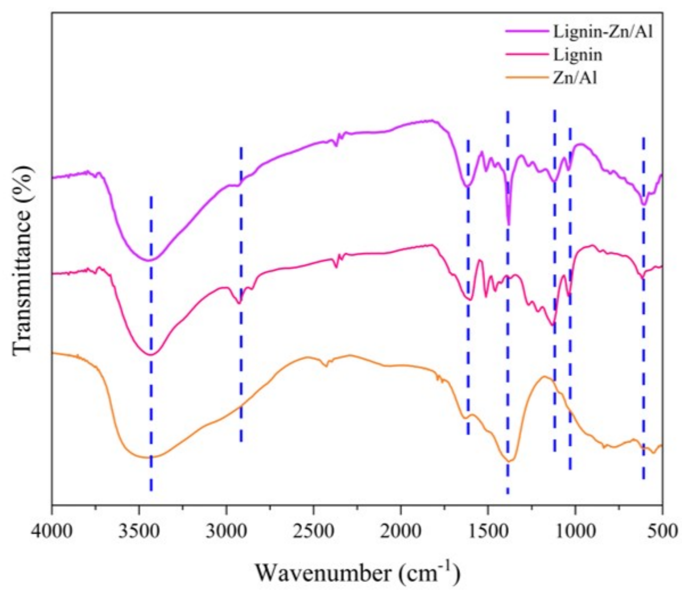

Figure 1. Fourier Transfer Infra-Red Results of Adsorbents

The usual Zn/Al XRD pattern can be seen in Figure 2, where the characteristic peaks are located at 10.1° and 20.1°, respectively, and correspond to the basal spacings of d003 and d006, respectively (Yuliasari et al., 2023). The 101 and 110 planes are responsible for two further linked peaks at 29.4° and 60.4°, respectively. The XRD of the lignin is depicted in Figure 2 and displays the distinctive peak of carbon material at 19.1° and 33.9° (Sturgeon et al., 2014). The XRD results of the lignin-Zn/Al mixture reveal the presence of distinctive Zn/Al and lignin reflections.

When evaluating the lignin-Zn/Al structure, the specific surface area and pore size are important factors. Table 3 quantitatively displays the lignin-Zn/Al, lignin, and Zn/Al pore's structure (d), surface area (S_{BET}), and pore volume (VP). The

Table 1. The Surface Area of Adsorbents

Adsorbent	S_{BET} (m^2/g)	d (nm)	VP (cm^3/g)
Lignin-Zn/Al	7.125	1.960	0.007
Lignin	4.079	2.255	0.009
Zn/Al	1.968	27.687	0.006

Table 2. Kinetic Data of Adsorbents

Adsorbent		Pseudo-First-Order			Pseudo-Second-Order		
	Qe_{exp} (mg/g)	Qe_{calc} (mg/g)	k_1 (min^{-1})	R^2	Qe_{calc} (mg/g)	k_2 (g/mg.min)	R^2
Lignin-Zn/Al	45.642	17.527	0.024	0.850	47.170	0.002	0.999
Lignin	39.892	29.336	0.036	0.941	44.053	0.002	0.993
Zn/Al	36.148	39.455	0.037	0.995	39.683	0.002	0.996

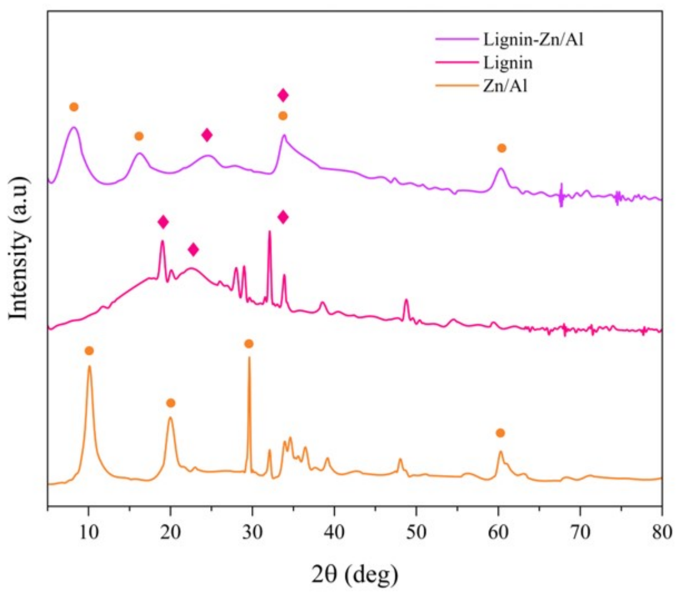

Figure 2. X-Ray Diffractometer Results of Adsorbents

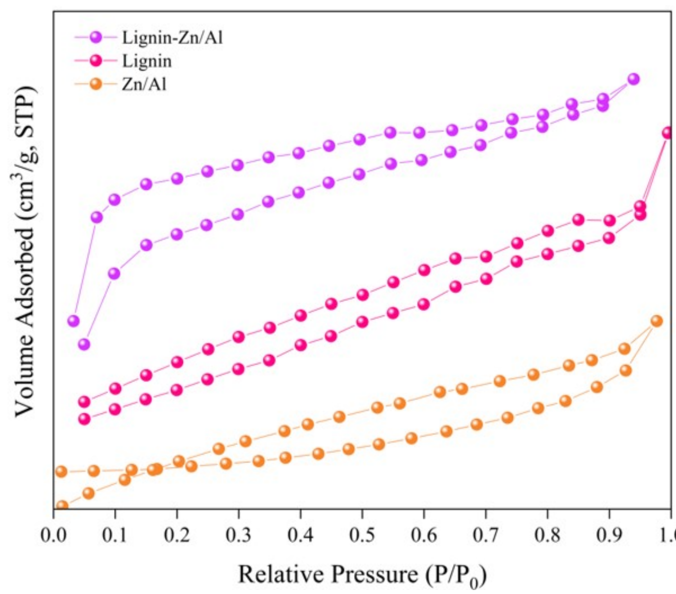

Figure 3. Nitrogen Adsorption-Desorption Results of Adsorbents

results show that lignin-Zn/Al has an average surface area of 7.125 m^2/g and pore sizes of 1.9620 ≈ 2 nm. The surface area of Zn/Al increase after combining with lignin. Our findings demonstrate the presence of mesopores in the lignin-Zn/Al structure, which have IUPAC-recommended diameter ranges of 2–50 nm (Heo et al., 2022). The N_2 adsorption/desorption curves and BJH (Barrett, Joyner, Halenda) pore size distributions of lignin-Zn/Al are shown in Figure 2. The lignin-Zn/Al nitrogen adsorption-desorption isotherm, as reported by IUPAC, showed a Type-IV curve, indicating that it had a mesoporous structure. The H3 kind of hysteresis loop also provides evidence for the presence of mesopores within the lignin-Zn/Al complex.

The pHpzc of is the point when there is no charge at all. When the pH of the solution is low, shaking causes H^+ to migrate from the solution to the surface of the lignin-Zn/Al, lignin, and Zn/Al, raising the pH. When the solution has a high pH, H^+ diffuses into the solution from the surface of lignin-Zn/Al, lignin, and Zn/Al. This reduces the pH of the solution. H^+ ions do not migrate at the point where the initial and final pHs meet, indicating that pHpzc is the point of convergence. Lignin-Zn/Al, lignin, and Zn/Al had pHpzc values of 6.09, 3.01, and 6.09, respectively, as illustrated in Figure 4. Lignin-Zn/Al, lignin, and Zn/Al are positively charged when the pH of the solution is less than pHpzc, and they are negatively charged when the pH of the solution is more than pHpzc .

Table 2 lists the resulting parameters after the experimental

Table 3. Isotherm Data of MG Adsorption

Adsorbent	T (°C)	Freundlich			Langmuir		
		n	kF	R^2	Qmax	kL	R^2
Lignin-Zn/Al	30	5.230	1.431	0.828	78.125	0.233	0.994
	40	5.959	1.452	0.781	79.365	0.341	0.995
	50	7.930	1.490	0.645	83.333	0.723	0.996
	60	1.101	1.506	0.668	84.034	1.469	0.999
Lignin	30	1.978	1.228	0.878	67.568	0.076	0.955
	40	2.033	1.244	0.882	71.942	0.075	0.917
	50	2.439	1.291	0.928	72.464	0.093	0.985
	60	2.475	1.309	0.947	78.740	0.102	0.981
Zn/Al	30	0.876	2.037	0.880	23.310	0.121	0.982
	40	1.071	1.903	0.763	26.954	0.155	0.954
	50	1.388	1.789	0.732	30.675	0.203	0.956
	60	1.916	1.684	0.778	36.364	0.342	0.980

Table 4. Several Adsorbents to the Adsorption of MG

Adsorbent	Qmax (mg/g)	References
Lignin-Zn/Al	84.034	This study
Lignin	78.740	This study
Zn/Al	36.364	This study
Avena sativa	83	Banerjee et al. (2016)
Pine cone	111.1	Kavci (2021)
Graphene oxide aminated lignin aerogels	113.5	Chen et al. (2020)
Halloysite nanotube	74.95	Altun and Ecevit (2022)
Active carbons	58	Hijab et al. (2021)
Chitosan-zink oxide	11	Muinde et al. (2020)
PACT@γ-Fe_2O_3	62.89	Hasan et al. (2020)

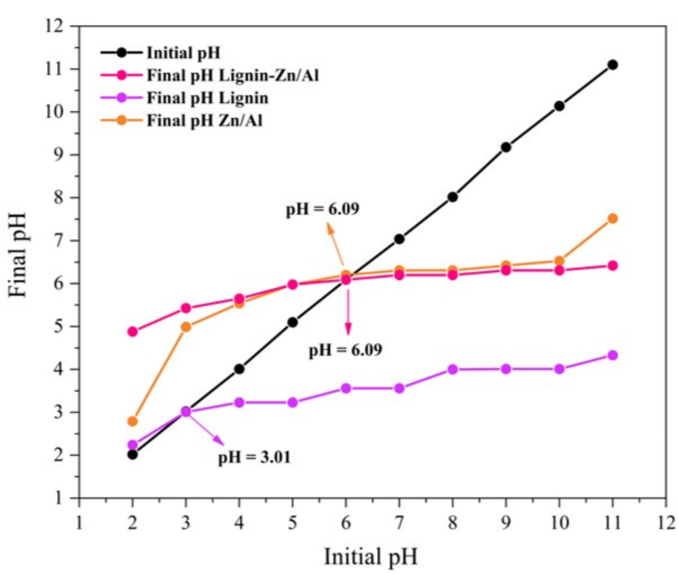

Figure 4. pHpzc of Lignin-Zn/Al, Lignin, and Zn/Al

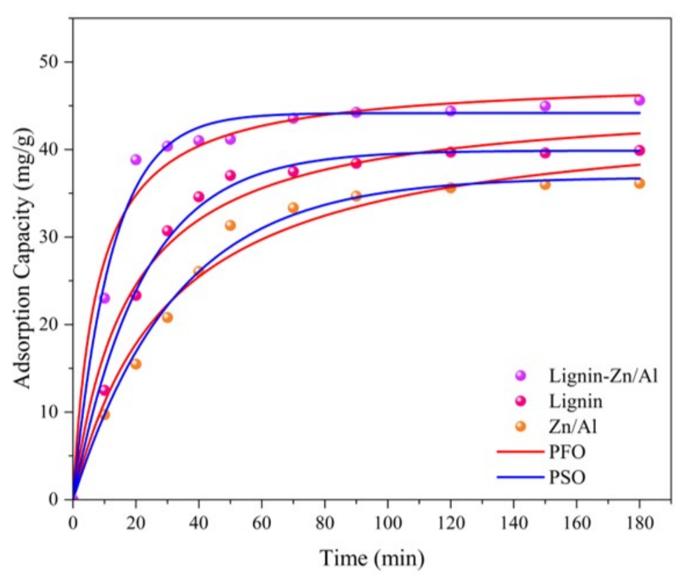

Figure 5. Contact Time Between Adsorbents and Adsorbate

data are fitted to the kinetics models. The pseudo-second-order equation is the most appropriate one to describe the adsorption kinetics of lignin-Zn/Al, lignin, Zn/Al for MG, as shown by the analysis of correlation coefficients shown in Table 2. All R^2 of the pseudo-second-order models are much closer to 1.0 than pseudo-first-order models. This suggests that the process of adsorption involves chemisorption (Rashed et al., 2022).

Isotherm studies were carried out to comprehend the MG adsorption equilibrium distribution between the aqueous and the lignin-Zn/Al, lignin, and Zn/Al phases. Due to their widesp read acceptance and popularity for precisely characterizing adsorption processes, the Langmuir and Freundlich models were used to explain the adsorption process in order to achieve that. The parameters obtained after fitting the isotherm research data obtained at various temperatures into these models are shown in Table 3. The Langmuir model best represented the MG adsorption onto all adsorbents, according to the R^2 values for the three adsorbents. It follows that monolayer adsorption in nature Meng et al. (2019) would be a more accurate way to characterize the MG solution's adsorption onto lignin-Zn/Al, lignin, and Zn/Al. The lignin-Zn/Al, lignin, and Zn/Al were shown to have maximum Langmuir adsorption capacities of 83.034, 78.740, and 36.364 mg/g, respectively. Zn/Al adsorption capacity increased 2.28 times after being composited with lignin. Several adsorbents for the adsorption of MG are displayed in Table 4.

4. CONCLUSION

Preparation lignin-Zn/Al is successful by the coprecipitation method. The characterization by FTIR, XRD, and BET shows the physicochemical characteristics of lignin-Zn/Al. The adsorption process showed better results after Zn/Al and lignin were combined. This can be seen from the increase in the adsorption capacity of Zn/Al lignin by 2.28 times. Thus, lignin-Zn/Al can be one of the adsorbents for the malachite green adsorption process.

5. ACKNOWLEDGMENT

The authors acknowledge to Research Center of Inorganic Materials and Complexes, FMIPA Universitas Sriwijaya for the support of this work.

REFERENCES

Ahmad, N., F. S. Arsyad, I. Royani, and A. Lesbani (2023a). Charcoal Activated as Template Mg/Al Layered Double Hydroxide for Selective Adsorption of Direct Yellow on Anionic Dyes. *Results in Chemistry*, **5**(1); 100766

Ahmad, N., F. S. Arsyad, I. Royani, P. M. S. B. N. Siregar, T. Taher, and A. Lesbani (2023b). High Regeneration of ZnAl/NiAl-Magnetite Humic Acid for Adsorption of Congo Red from Aqueous Solution. *Inorganic Chemistry Communications*, **150**; 110517

Ahmed, M. A. and A. A. Mohamed (2022). A Systematic Review of Layered Double Hydroxide-based Materials for Environmental Remediation of Heavy Metals and Dye Pollutants. *Inorganic Chemistry Communications*, **148**; 110325

Altun, T. and H. Ecevit (2022). Adsorption of Malachite Green and Methyl Violet 2B by Halloysite Nanotube: Batch Adsorption Experiments and Box-behnken Experimental Design. *Materials Chemistry and Physics*, **291**; 126612

Banerjee, S., G. C. Sharma, R. K. Gautam, M. Chattopadhyaya, S. N. Upadhyay, and Y. C. Sharma (2016). Removal of Malachite Green, A Hazardous Dye from Aqueous Solutions Using Avena Sativa (oat) Hull as A Potential Adsorbent. *Journal of Molecular Liquids*, **213**; 162–172

Buvaneswari, K. and M. Singanan (2022). Removal of Malachite Green Dye In Synthetic Wastewater Using Zingiber Officinale Plant Leaves Biocarbon. *Materials Today: Proceedings*, **55**; 274–279

Chen, H., T. Liu, Y. Meng, Y. Cheng, J. Lu, and H. Wang (2020). Novel Graphene Oxide/Aminated Lignin Aerogels for Enhanced Adsorption of Malachite Green in Wastewater. *Colloids and Surfaces A: Physicochemical and Engineering Aspects*, **603**; 125281

Chen, Y., S. Chen, Z. Deng, X. Xu, J. Qin, X. Guo, Z. Bai, X. Chen, and Z. Lu (2022). Fabrication of Polystyrene/Cuo@ Calcined Layered Double Hydroxide Microspheres with High Adsorption Capacity for Congo Red. *Colloids and Surfaces A: Physicochemical and Engineering Aspects*, **652**; 129827

Dahlan, I., O. H. Keat, H. A. Aziz, and Y. T. Hung (2023). Synthesis and Characterization of MOF-5 Incorporated Waste-derived Siliceous Materials for the Removal of Malachite Green Dye From Aqueous Solution. *Sustainable Chemistry and Pharmacy*, **31**; 100954

Du, B., W. Li, L. Chai, W. Li, X. Wang, X. Chen, J. Zhou, and R. C. Sun (2023). Preparation of Versatile Lignin-based Adsorbent for The Removal of Organic Dyes and Its Application in Wound Healing. *Journal of Molecular Liquids*, **377**; 121566

Giri, B. S., R. K. Sonwani, S. Varjani, D. Chaurasia, T. Varadavenkatesan, P. Chaturvedi, S. Yadav, V. Katiyar, R. S. Singh, and A. Pandey (2022). Highly Efficient Bio-adsorption of Malachite Green Using Chinese Fan-palm Biochar (livistona Chinensis). *Chemosphere*, **287**; 132282

Hamad, H. A., S. AbdElhafez, M. Elsenety, M. K. Sorour, N. Amin, O. Abdelwahab, and E. Z. El Ashtoukhy (2022). Fabrication and Characterization of Functionalized Lignin-based Adsorbent Prepared from Black Liquor in the Paper Industry for Superior Removal of Toxic Dye. *Fuel*, **323**; 124288

Hasan, I., D. Bhatia, S. Walia, and P. Singh (2020). Removal of Malachite Green by Polyacrylamide-g-chitosan γ-Fe_2O_3 Nanocomposite-an Application of Central Composite Design. *Groundwater for Sustainable Development*, **11**; 100378

Heo, J. W., L. An, J. Chen, J. H. Bae, and Y. S. Kim (2022). Preparation of Amine-functionalized Lignins for the Selective Adsorption of Methylene Blue and Congo Red. *Chemosphere*, **295**; 133815

Hijab, M., P. Parthasarathy, H. R. Mackey, T. Al Ansari, and G. McKay (2021). Minimizing Adsorbent Requirements Using Multi-stage Batch Adsorption for Malachite Green Removal Using Microwave Date-stone Activated Carbons. *Chemical Engineering and Processing-Process Intensification*, **167**; 108318

Iqbal, A., E. Cevik, A. Bozkurt, S. M. M. Asiri, O. Alagha, T. F. Qahtan, M. I. Jalees, and M. U. Farooq (2022). Ultrahigh Adsorption by Regenerable Iron-cobalt Core-shell Nanospheres and Their Synergetic Effect on Nanohybrid Membranes for Removal Of Malachite Green Dye. *Journal of Environmental Chemical Engineering*, **10**(3); 107968

Jin, C., Y. Liu, J. Fan, T. Liu, G. Liu, F. Chu, and Z. Kong (2022). Lignin-inspired Porous Polymer Networks as High-performance Adsorbents for the Efficient Removal of Malachite Green Dye. *Colloids and Surfaces A: Physicochemical and Engineering Aspects*, **643**; 128760

Juleanti, N., N. R. Palapa, T. Taher, N. Hidayati, B. I. Putri, and A. Lesbani (2021). The Capability of Biochar-based CaAl and MgAl Composite Materials as Adsorbent For Removal Cr (VI) in Aqueous Solution. *Science and Technology Indonesia*, **6**(3); 196–203

Kavci, E. (2021). Malachite Green Adsorption Onto Modified Pine Cone: Isotherms, Kinetics and Thermodynamics Mechanism. *Chemical Engineering Communications*, **208**(3); 318–327

Meng, Z., M. Wu, S. Zhao, R. Jing, S. Li, Y. Shao, X. Liu, F. Lv, A. Liu, and Q. Zhang (2019). Removing Anionic Dyes from Wastewater Based on In-situ Formation Of Fe_3O_4@ Zn-Al Layered Double Hydroxides by Self-assembly. *Applied Clay Science*, **170**; 41–45

Moradi, O. and S. Panahandeh (2022). Fabrication of Different Adsorbents Based on Zirconium Oxide, Graphene Oxide, and Dextrin for Removal of Green Malachite Dye from Aqueous Solutions. *Environmental Research*, **214**; 114042

Muinde, V. M., J. M. Onyari, B. Wamalwa, and J. N. Wabomba (2020). Adsorption of Malachite Green Dye From Aqueous Solutions Using Mesoporous Chitosan–zinc Oxide Composite Material. *Environmental Chemistry and Ecotoxicology*, **2**; 115–125

Nazir, M. A., T. Najam, S. Jabeen, M. A. Wattoo, M. S. Bashir, S. S. A. Shah, and A. ur Rehman (2022). Facile Synthesis of Tri-metallic Layered Double Hydroxides (NiZnAl-LDHs): Adsorption of Rhodamine-B and Methyl Orange from Water. *Inorganic Chemistry Communications*, **145**; 110008

Pathania, D., V. S. Bhat, J. M. Shivanna, G. Sriram, M. Kurkuri, and G. Hegde (2022). Garlic Peel Based Mesoporous Carbon Nanospheres for an Effective Removal of Malachite Green Dye from Aqueous Solutions: Detailed Isotherms and Kinetics. *Spectrochimica Acta Part A: Molecular and Biomolecular Spectroscopy*, **276**; 121197

Puthukkara, P., A. Rose, T. S. Jose, and S. D. Lal (2022). Green Synthesis of Iron Nanoparticles for Malachite Green Removal. *Materials Today Communications*, **33**(4); 50–60

Rashed, S. H., A. Abd Elhamid, S. Y. H. Abdalkarim, R. H. El Sayed, A. A. El Bardan, H. M. Soliman, and A. Nayl (2022). Preparation and Characterization of Layered Double Hydroxides Decorated on Graphene Oxide For Dye Removal from Aqueous Solution. *Journal of Materials Research and Technology*, **17**; 2782–2795

Raval, A. R., H. P. Kohli, and O. K. Mahadwad (2022). Application of Emulsion Liquid Membrane for Removal of Malachite Green Dye from Aqueous Solution: Extraction and Stability Studies. *Chemical Engineering Journal Advances*, **12**; 100398

Ren, Q., C. Kong, Z. Chen, J. Zhou, W. Li, D. Li, Z. Cui, Y. Xue, and Y. Lu (2021). Ultrasonic Assisted Electrochemical Degradation of Malachite Green In Wastewater. *Microchemical Journal*, **164**; 106059

Sarkar, S., N. Tiwari, A. Basu, M. Behera, B. Das, S. Chakrabortty, K. Sanjay, M. Suar, T. K. Adhya, and S. Banerjee (2021). Sorptive Removal of Malachite Green From Aqueous Solution by Magnetite/coir Pith Supported Sodium Alginate Beads: Kinetics, Isotherms, Thermodynamics and Parametric Optimization. *Environmental Technology & Innovation*, **24**; 101818

Sturgeon, M. R., M. H. O'Brien, P. N. Ciesielski, R. Katahira, J. S. Kruger, S. C. Chmely, J. Hamlin, K. Lawrence, G. B. Hunsinger, and T. D. Foust (2014). Lignin Depolymerisation by Nickel Supported Layered Double Hydroxide Catalysts. *Green Chemistry*, **16**(2); 824–835

Sun, Y., T. Wang, C. Han, X. Lv, L. Bai, X. Sun, and P. Zhang (2022). Facile Synthesis of Fe-modified Lignin-based Biochar for Ultra-fast Adsorption of Methylene Blue: Selective Adsorption and Mechanism Studies. *Bioresource Technology*, **344**; 126186

Tang, R., W. Hong, C. Srinivasakannan, X. Liu, X. Wang, and X. Duan (2022). A Novel Mesoporous Fe-silica Aerogel Composite with Phenomenal Adsorption Capacity for Malachite Green. *Separation and Purification Technology*, **281**; 119950

Van Tran, T., D. T. C. Nguyen, P. S. Kumar, A. T. M. Din, A. S. Qazaq, and D. V. N. Vo (2022). Green Synthesis of Mn_3O_4 Nanoparticles Using Costus Woodsonii Flowers Extract for Effective Removal of Malachite Green Dye. *Environmental Research*, **214**; 113925

Vigneshwaran, S., P. Sirajudheen, P. Karthikeyan, and S. Meenakshi (2021). Fabrication of Sulfur-doped Biochar Derived from Tapioca Peel Waste with Superior Adsorption Performance for the Removal of Malachite Green and Rhodamine B Dyes. *Surfaces and Interfaces*, **23**; 100920

Wang, T., M. Jiang, X. Yu, N. Niu, and L. Chen (2022). Application of Lignin Adsorbent in Wastewater Treatment: A Review. *Separation and Purification Technology*, **302**; 122116

Wang, T., C. Li, C. Wang, and H. Wang (2018). Biochar/MnAl-LDH Composites for Cu (II) Removal from Aqueous Solution. *Colloids and Surfaces A: Physicochemical and Engineering Aspects*, **538**; 443–450

Yuliasari, N., A. Wijaya, R. Mohadi, and A. Lesbani (2023). Enhanced Effectiveness on Phenol Removal by MgCr-

LDH/Microcrystalline Cellulose Composite and Regeneration Study with Green Desorption Reagent. *Science and Technology Indonesia*, **8**(1); 151–159

Zong, E., R. Fan, H. Hua, J. Yang, S. Jiang, J. Dai, X. Liu, and P. Song (2023). A Magnetically Recyclable Lignin-based Bio-adsorbent for Efficient Removal of Congo Red From Aqueous Solution. *International Journal of Biological Macromolecules*, **226**; 443–453

Zubair, M., H. A. Aziz, I. Ihsanullah, M. A. Ahmad, and M. A. Al Harthi (2022). Engineered Biochar Supported Layered Double Hydroxide-cellulose Nanocrystals Composite-: Synthesis, Characterization and Azo Dye Removal Performance. *Chemosphere*, **307**; 136054